Acta Biochimica Indonesiana

https://doi.org/10.32889/actabioina.221

RESEARCH ARTICLE

Open Access

Photosynthetic efficiency and acid tolerance in *Pumiliosphaera acidicola* KMJ isolated from a geothermal spring in West Java, Indonesia

Alfredo Kono[1,2*], Berliana Gita N. Pertiwi[1], Bahzad Ahmad Farhan[1], Anhar Rahmawan[1], Yanti Rachmayanti[1], Rindia M. Putri[1], Zeily Nurachman[1]

[1]Biochemistry and Biomolecular Engineering Research Division, Faculty of Mathematics and Natural Sciences, Institut Teknologi Bandung, Jl. Ganesha 10, Bandung, West Java, Indonesia, 40132

[2]Bioscience and Biotechnology Research Center, Institut Teknologi Bandung, Jl. Ganesha 10, Bandung, West Java, Indonesia, 40132

[*]Corresponding author: Jl. Ganesha 10, Bandung, West Java, Indonesia, 40132. Email: akono@itb.ac.id

ABSTRACT

Background: Acidophilic microalgae represent a promising yet underexplored resource for biotechnological carbon capture in low-pH environments such as geothermal springs and industrial effluents. However, few strains have been physiologically characterized, and most biotechnologically relevant microalgae remain neutrophilic.

Objective: This study aimed to isolate and characterize an acid-tolerant green microalga from a geothermal spring in Kamojang, West Java, Indonesia, and assess its growth, acid tolerance, and photosynthetic performance across a range of inorganic carbon (C_i: CO_2, HCO_3^-, and CO_3^{2-}) concentrations.

Methods: Mud samples were enriched in Allen medium under continuous illumination. Isolates were identified via 18S rRNA sequencing and phylogenetic analysis. Growth was tested across pH 2.3 to 7.0 in media acidified with either HCl or H_2SO_4. Photosynthetic performance was evaluated by O_2 evolution under various C_i concentrations.

Results: The isolated strain, designated *Pumiliosphaera acidicola* KMJ, exhibited robust growth from pH 2.3 to 7.0 and showed comparable tolerance to both HCl and H_2SO_4. Morphologically, KMJ displayed compact, spherical green cells (2–5 µm diameter). Oxygen evolution measurements revealed consistently higher photosynthetic rates than *Chlamydomonas reinhardtii*, particularly under sub-saturating Ci levels, indicating efficient CO_2 assimilation under acidic, low-Ci conditions. To our knowledge, this is the first study to directly quantify C_i-dependent O_2 evolution in an acidophilic chlorophyte.

Conclusion: *P. acidicola* KMJ combines broad acid tolerance with high photosynthetic efficiency, positioning it as a strong candidate for CO_2 capture in acidic environments. Its physiology also provides a basis for future molecular studies into acidophilic CO_2 assimilation.

Keywords: acidophilic microalgae, CO_2 capture, geothermal spring, photosynthesis, *Pumiliosphaera acidicola*.

Introduction

Rising atmospheric carbon dioxide (CO_2) concentrations—now exceeding 420 ppm—are a major driver of global climate change, with wide-ranging impacts on terrestrial and aquatic ecosystems [1-3]. This persistent increase, driven primarily by anthropogenic emissions, has prompted urgent development of effective carbon management strategies. Among natural CO_2 sinks, photosynthesis remains the most critical biological mechanism for CO_2 sequestration, converting inorganic carbon into organic biomass through the Calvin–Benson–Bassham (CBB) cycle. This pathway assimilates approximately 120 gigatons of CO_2 annually and functions as a vital buffer in the global carbon cycle. Aquatic photoautotrophs—including phytoplankton and microalgae—are responsible for nearly half of this global CO_2 fixation [4].

Microalgae, in particular, offer significant promise for sustainable CO_2 mitigation due to their high photosynthetic efficiency, rapid growth rates, and adaptability to diverse cultivation systems [5, 6].

However, most species investigated to date are neutrophilic, favoring growth at pH 6.5–8.0 [6-8]. This pH dependency constrains large-scale applications, especially in extreme or non-sterile environments. In contrast, acidic habitats offer several advantages for CO_2 sequestration. For instance, at pH 4, dissolved molecular CO_2 can be up to ten times more abundant than at neutral pH due to shifts in carbonate equilibrium [9]. These environments also exhibit lower microbial contamination risks and exert unique ecological pressures—such as high proton and metal ion concentrations—that may drive evolution of specialized carbon assimilation traits [10]. These characteristics make acidophilic microalgae promising, yet largely underexplored, candidates for biotechnological applications in low-pH systems such as industrial effluents and geothermal environments.

Despite this potential, few acid-tolerant microalgal strains have been isolated or functionally characterized. Compared to previous isolation efforts in geothermal and acidic environments—such as acid mine drainages [11] and temperate springs in Europe and North America [12]—this study targets the volcanically active Indonesian archipelago, providing geographically distinct isolates and novel insights into the ecological traits of Southeast Asian acidophilic chlorophytes. Indonesia's geothermal regions, shaped by more than 100 active volcanoes and widespread hot spring systems, offer an exceptional but underutilized source of acid-adapted microalgae. These habitats are frequently characterized by acidic waters with high concentrations of dissolved metals and sulfate, creating extreme physicochemical conditions that may serve as strong selective pressures for the evolution of acid-tolerant and metal-resistant microalgal lineages [13, 14]. In particular, native chlorophytes inhabiting these low-pH environments remain poorly studied, limiting both our ecological understanding and the development of acidophilic production strains for CO_2 capture.

In this study, we report the isolation and characterization of an acidophilic green microalga from a geothermal spring in Kamojang, West Java. The isolate, designated *Pumiliosphaera acidicola* KMJ, was evaluated for pH tolerance, acid source adaptability, and photosynthetic performance under varying inorganic carbon (C_i: CO_2, HCO_3^-, and CO_3^{2-}) concentrations. These traits were compared to those of the model neutrophilic alga *Chlamydomonas reinhardtii* to assess the potential of KMJ for biotechnological CO_2 capture in low-pH environments.

Methods

Sampling, microalgae isolation, and regular maintenance

Mud samples were collected from the surface layer (approximately 10 cm in depth) of a geothermal spring in Kamojang, West Java, Indonesia (coordinates: -7.12487, 107.79998) using plastic bottles, with a total sample volume of approximately 500 mL. Upon arrival at the laboratory, 15 mL of the mud was suspended in 25 mL of 1× Allen medium. Allen medium was selected due to its prior use in cultivating acidophilic microalgae such as *Cyanidium caldarium* and *Galdieria sulphuraria* [15, 16], making it a suitable choice for enriching low-pH adapted strains. The mud and 1× Allen medium were mixed thoroughly in 50 mL Falcon tubes and left undisturbed at room temperature for 15 minutes to allow sedimentation. Subsequently, 1 mL of the supernatant and 500 µL of the sediment were each transferred into separate flasks containing 25 mL of fresh 1× Allen medium. The cultures were incubated under continuous illumination at 100 µmol photons m^{-2} s^{-1} and agitated at 150 rpm. Gradual development of green coloration was observed within one month, indicating progressive enrichment of photosynthetic microalgae.

To eliminate bacterial and fungal contaminants, cultures were physically washed through repeated cycles of centrifugation and resuspension in sterile 1× Allen medium. Fifty milliliters of culture was centrifuged at 3000 rpm for 15 minutes, the resulting pellets were resuspended in 25 mL of sterile 1× Allen medium, and the process was repeated five times. Following the final wash, cultures were

serially diluted in 100 mL Erlenmeyer flasks containing fresh 1× Allen medium and incubated under identical conditions for 24 hours.

On the following day, 5 µL of each culture was spotted onto solid Allen medium plates to assess microbial contamination. Washing and plating steps were repeated until no visible bacterial or fungal growth was observed. Axenic cultures were then streaked on solid Allen medium to isolate single colonies, which were subsequently transferred into fresh liquid Allen medium for further analysis. Axenicity was confirmed by repeated streaking and visual inspection under light microscopy; no molecular screening for bacterial or fungal contaminants was conducted. Isolated strains were routinely maintained on solid Allen medium at pH 4, the lowest feasible pH for agar-based cultivation according to our laboratory observations, as solid media could not be prepared reliably below this threshold. Based on our experience, agar solidification consistently failed at pH values below approximately 4, likely due to acid- and heat-induced hydrolysis of the gel matrix, consistent with previous reports [17].

Growth studies in different pH values

To evaluate growth under different acidic conditions and acid sources, 1× Allen medium was adjusted to the desired pH using either HCl or H_2SO_4. As the native pH of 1× Allen medium is approximately 5, pH adjustments to near-neutral conditions (pH 6 and pH 7) were made using NaOH. Equal cell densities were used to inoculate both solid and liquid cultures. For liquid cultures, cell concentrations were determined using a hemocytometer, following a previously described protocol with technical replicates [18].

Microscopic measurement of cell size

Cell size was estimated from bright-field micrographs captured at 40× magnification using a hemocytometer grid with known dimensions of 1 mm × 1 mm. A reference image containing 0.2 mm × 0.2 mm grid squares was used to establish the pixel-to-micrometer conversion factor (1 pixel ≈ 0.98 µm). Cell diameters were determined by detecting individual cells through adaptive thresholding and contour-based image analysis using ImageJ software (version 1.53; National Institutes of Health, USA). To eliminate background artifacts and multicellular aggregates, only objects with estimated diameters between 2 and 20 µm were included. A total of 4,119 individual cells were analyzed. Inter-observer variability was assessed using 100 randomly selected cells, with two independent observers performing measurements. The mean percentage difference was less than 5%, indicating high consistency in cell size estimates.

18S rRNA gene amplification

Genomic DNA from individual algal colonies was extracted using 5% Chelex (Sigma) following a previously described protocol [18, 19]. The 18S rRNA gene was amplified by PCR using GoTaq® Green Master Mix (Promega) with the following primers: forward primer 18S M13F (5′-TGTAAAACGACGGCCAGTATTCCAGCTCCAATAGG-3′) and reverse primer 18S M13R (5′-CAGGAAA CGCTATGACGGACTACGATGGTATCTAATC-3′). These primers target the hypervariable V4 region of the 18S rRNA gene. The PCR procedure followed the manufacturer's protocol, with an annealing temperature of 50 °C. PCR products were subjected to Sanger sequencing by Apical Scientific Sequencing (Selangor, Malaysia).

Bioinformatics analysis of algal sequence

Sequencing results were aligned using Clustal Omega (EMBL-EBI) for multiple sequence alignment [20]. The alignment was visualized using MView. Phylogenetic analysis of 18S rRNA sequences was performed using MrBayes v3.2.7 [21]. Sequences were aligned using Clustal Omega and saved in NEXUS format. Bayesian inference was conducted using the GTR model with gamma-distributed rate variation across sites (GTR+G). Two independent Markov Chain Monte Carlo (MCMC) runs were executed with four chains each, running for 1,000,000 generations and sampling every 100 generations.

The first 25% of samples were discarded as burn-in. Convergence was assessed by monitoring the average standard deviation of split frequencies and effective sample size (ESS) values. Posterior probabilities were calculated to evaluate support for each node. FigTree software was used to visualize the resulting phylogenetic trees [22].

Photosynthetic O_2 evolution assay

To assess photosynthetic activity, cells of the newly isolated algal strain were grown in liquid 1× Allen medium adjusted to pH 4 with HCl, under continuous illumination (100 µmol photons m^{-2} s^{-1}) and ambient air (~0.04% CO_2). For comparison, the photosynthetic activity of the model alga *C. reinhardtii* (strain CC5370) was also evaluated. *C. reinhardtii* cells were initially grown in liquid TAP medium until mid-log phase, then transferred to Tris-Minimal Medium for 24 hours under ambient air to induce the CO_2-concentrating mechanism (CCM). TAP medium and Tris-Minimal Medium were prepared as previously described [23].

For the photosynthetic O_2 evolution assay, cells were harvested by centrifugation at 3000 rpm for 5 minutes at room temperature and resuspended in 25 mM MES-KOH buffer (pH 6). Cell suspensions were adjusted to equivalent chlorophyll concentrations, as determined spectrophotometrically [24]. Each assay was performed using 2 mL of the prepared cell suspension.

Photosynthetic O_2 evolution was measured using a Clark-type oxygen electrode system (OxyLab, Hansatech Instruments, UK) at 25 °C as previously described [18]. Prior to measurement, cells were pre-illuminated at 500 µmol photons m^{-2} s^{-1} until endogenous inorganic carbon (C_i: CO_2, HCO_3^-, CO_3^{2-}) was exhausted, as indicated by cessation of O_2 evolution. The assay was initiated by adding exogenous C_i in the form of $NaHCO_3$ to determine C_i-dependent O_2 evolution. Measurements were recorded only after the complete consumption of C_i from the previous addition, as confirmed by a drop in O_2 evolution to baseline levels. To minimize potential inhibition of photosynthesis from elevated O_2 concentrations, the chamber was flushed with N_2 gas when O_2 levels exceeded 200 nmol mL^{-1}. Photosynthetic O_2 evolution was normalized per mg chlorophyll to ensure comparability between strains.

Results

Microalga isolation and strain confirmation

Sediment and supernatant fractions of mud samples collected from a geothermal spring in Kamojang, West Java, Indonesia, developed a distinct green coloration after approximately one month of cultivation in 1× Allen medium under continuous high light, indicating successful enrichment of microalgal populations (**Figure 1**A, D). Following a series of washing steps and spot plating on solid Allen medium (see Methods), we obtained axenic cultures free of bacterial and fungal contamination. Subsequent streaking yielded discrete green colonies from both sediment- and supernatant-derived samples (**Figure 1**B-F).

To verify the identity of the isolates, we selected four representative colonies—two from each source—for partial 18S rRNA gene sequencing. PCR amplification produced ~500 bp products from all samples. Sanger sequencing chromatograms displayed single, sharp peaks throughout the region, confirming that each sample originated from a genetically uniform culture derived from a single colony-forming cell. Genetic uniformity was assessed by visual inspection of the resulting chromatograms. Sequence alignment revealed 100% identity between the sequences from sediment- and supernatant-derived isolates, suggesting that they belong to the same species (**Figure 2**).

Morphological examination conducted prior to 18S rRNA sequencing further supported this conclusion. No distinguishable morphological or growth differences were observed between isolates from sediment and supernatant fractions prior to genetic confirmation. Light microscopy revealed that all isolates exhibited small, spherical green cells typical of chlorophyte microalgae (**Figure 3**). Quantitative image analysis of 4,119 individual cells (see Methods) revealed diameters ranging from 2.19 µm to 19.90 µm, with a mean of 3.81 µm,

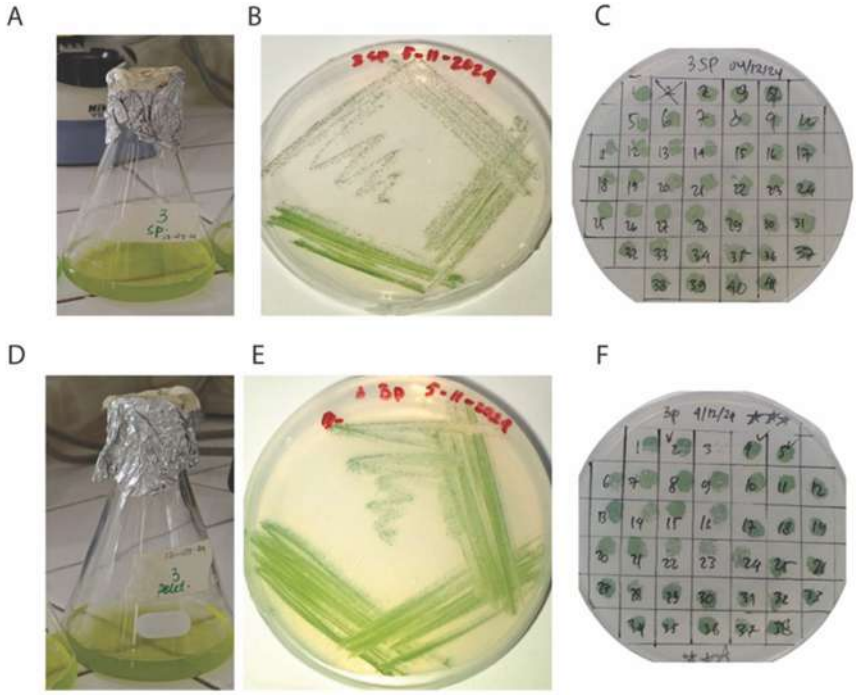

Figure 1. Enrichment and isolation of microalgae from geothermal mud samples. (A–C) Supernatant fraction; (D–F) sediment fraction. (A, D) Enriched cultures showing distinct green coloration after one month of incubation in 1× Allen medium under continuous illumination, indicating successful microalgal growth. (B, E) Streaking on solid 1× Allen medium to obtain single colonies from the enriched cultures. (C, F) Spot plating of isolated colonies showing uniform growth patterns; axenic status was confirmed through successive subculturing.

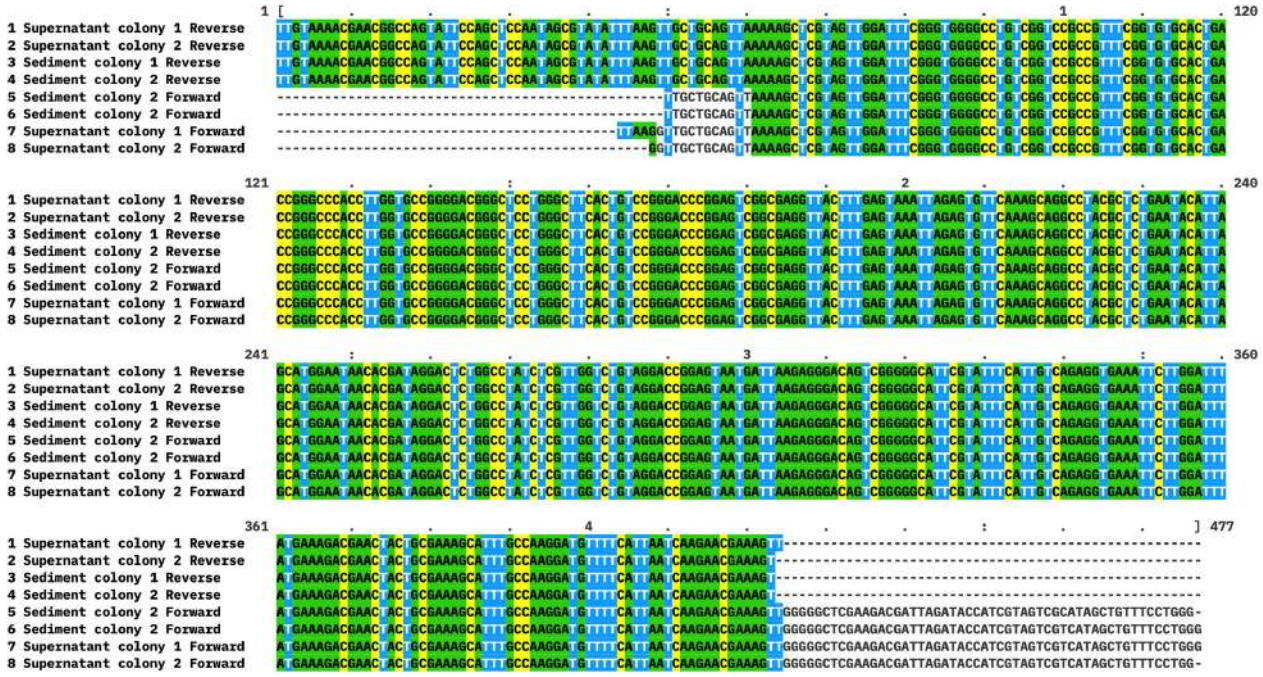

Figure 2. Sequence alignment of partial 18S rRNA genes from isolated microalgal colonies. Alignment of partial 18S rRNA gene sequences obtained from single colonies isolated from the sediment and supernatant fractions of geothermal mud. Sequences represent overlapping regions amplified using forward and reverse primers, confirming sequence identity between isolates from both sources.

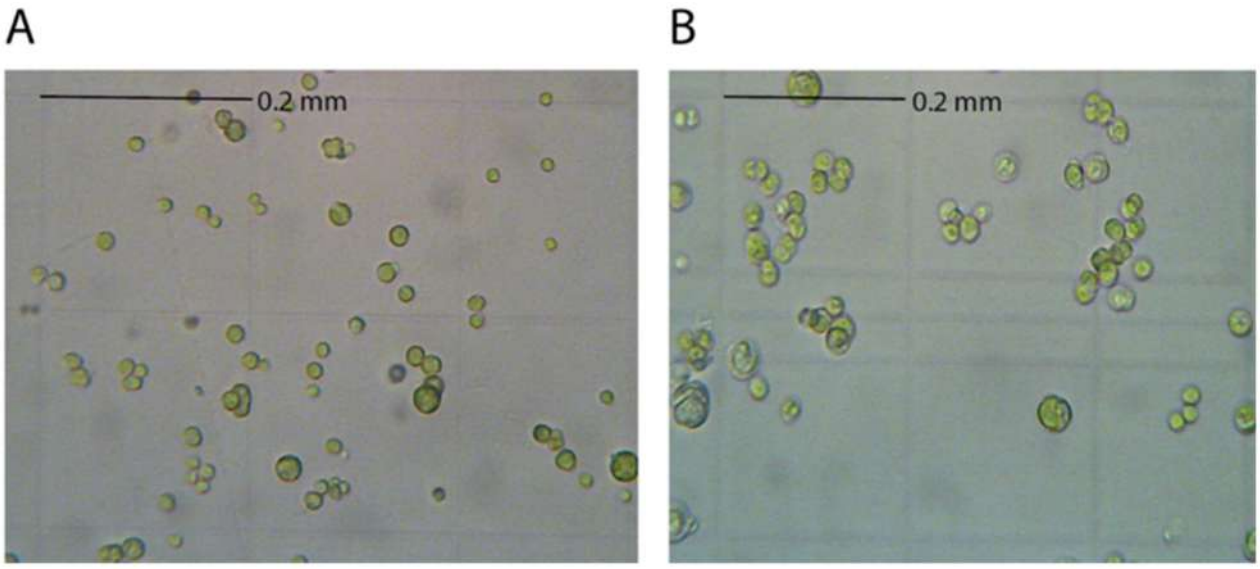

Figure 3. Morphological characterization of isolated microalgal cells. Light microscopy images of cells isolated from (A) sediment and (B) supernatant fractions of geothermal mud. Most cells fall within the 2–5 µm diameter range.

a median of 2.77 µm, and a standard deviation of 2.41 µm. The majority of cells fell within the 2–5 µm range, consistent with the typical size reported for *P. acidicola* [25], and supporting the identification subsequently confirmed by 18S rRNA sequencing.

To determine taxonomic identity, we performed BLAST analysis of the 18S rRNA gene sequences. All isolates showed highest similarity to *Auxenochlorella protothecoides* var. *acidicola*, with 99.72% sequence identity and 100% query coverage. We further assessed the evolutionary placement of the isolates by constructing a phylogenetic tree based on 18S rRNA sequences from a broad range of green algal, red algal, and diatom species. The resulting phylogeny positioned the isolates within the *A. protothecoides* var. *acidicola* clade, clustering closely with reference strains SAG1591, Cant1, and RSa5 (**Figure 4**). Notably, reference strain *A. protothecoides* var. *acidicola* strain SAG1951 has been reclassified under the newly established genus *Pumiliosphaera*, with *P. acidicola* designated as the type species based on conserved ITS-2 DNA barcode regions [25]. Accordingly, we designated our isolate as *Pumiliosphaera acidicola* strain KMJ (hereafter *P. acidicola* KMJ) with "KMJ" referring to its site of origin in Kamojang.

Although *P. acidicola* KMJ is nested within a broader phylogenetic assemblage that includes several *Chlorella* species, it is phylogenetically distinct from canonical *A. protothecoides*, supporting its classification as a separate varietal lineage. The *Auxenochlorella–Chlorella* cluster was clearly resolved from other green algal taxa such as *C. reinhardtii*, and from basal branches containing red algal species (*Galdieria sulphuraria*, *Cyanidium caldarium*). Diatom species (*Navicula trivialis* and *Cyclotella striata*) were used as outgroups to root the tree due to their well-documented evolutionary divergence from green algae [26].

Acid adaptability

To evaluate acid tolerance, we assessed the ability of the isolated KMJ strain to grow under acidic conditions using both solid and liquid 1× Allen media adjusted to various pH levels. On solid medium, the strain exhibited visible growth at pH 3, 4, and 5, even when inoculated at low initial cell densities, indicating a broad tolerance to acidic environments (**Figure 5**A).

We then assessed growth in liquid 1× Allen medium adjusted to pH 2.3, 3.3, and 4.1 using two acid sources: hydrochloric acid (HCl) and sulfuric acid (H_2SO_4). To test the strain's ability

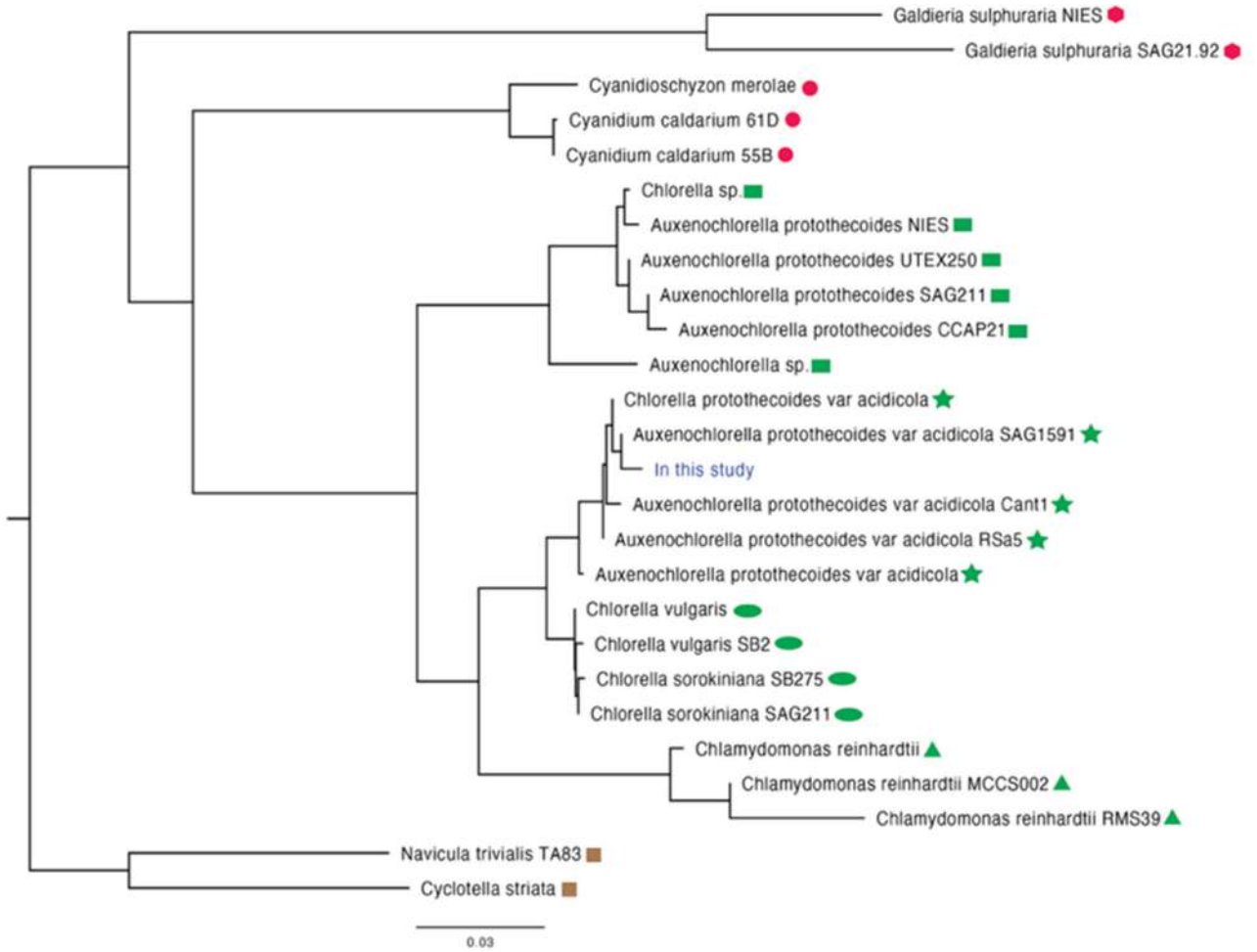

Figure 4. Phylogenetic analysis of *Pumiliosphaera acidicola* KMJ based on 18S rRNA gene sequences. Phylogenetic tree showing the placement of *Pumiliosphaera acidicola* KMJ (this study, labeled in blue) relative to selected green algae, red algae, and diatom species. Symbol colors indicate algal groups: green for green algae, red for red algae, and brown for diatoms. Symbol shapes represent different genera or species within each group. Diatoms (*Navicula trivialis* and *Cyclotella striata*) were used as outgroups. The scale bar indicates 0.04 substitutions per site. Accession numbers (in order): *Galdieria sulphuraria* NIES (LC504057.1), *Galdieria sulphuraria* SAG21.92 (AB091230.1), *Cyanidioschyzon merolae* (XR_002461579.1), *Cyanidium caldarium* 61D (AB090833.1), *Cyanidium caldarium* 55B (AB091232.1), *Chlorella* sp. (X72708.1), *Auxenochlorella protothecoides* NIES (AB488570.1), *Auxenochlorella protothecoides* UTEX250 (JN677643.1), *Auxenochlorella protothecoides* SAG211 (KM020150.1), *Auxenochlorella protothecoides* CCAP21 (FN298931.1), *Auxenochlorella* sp. (AM260449.1), *Chlorella vulgaris* (GU295219.1), *Chlorella vulgaris* SB2 (KX495015.1), *Chlorella sorokiniana* SB275 (KX495053.1), *Chlorella sorokiniana* SAG211 (X62441.2), *Chlamydomonas reinhardtii* (AB511837.1), *Chlamydomonas reinhardtii* MCCS002 (EF682842.2), *Chlamydomonas reinhardtii* RMS39 (KF750626.1), *Chlorella protothecoides* var. *acidicola* (AJ439399.2), *Auxenochlorella protothecoides* var. *acidicola* SAG1591 (LN610705.1), Cant1 (JF694006.1), RSa5 (KM016995.1), *Auxenochlorella protothecoides* var. *acidicola* (KM462820.1), *Navicula trivialis* (KY320372.1), and *Cyclotella striata* (JQ217342.1).

to grow under near-neutral conditions, additional cultures were prepared at pH 6.1 and 7.0 by adjusting the medium with NaOH. Cultures were incubated for 9 days, and cell concentrations were measured at the end of the experiment. The KMJ strain grew across all tested pH conditions, with no statistically significant differences in final cell densities (**Figure 5**B; two-way ANOVA, $p > 0.05$), demonstrating its capacity to thrive in a wide pH range from acidic to near-neutral.

No significant differences were observed between cell concentrations in HCl- and H_2SO_4-acidified media at each pH level (**Figure 5**B, two-way ANOVA, $p > 0.05$), suggesting that the strain is equally tolerant of chloride and sulfate ions. Interestingly, the strain failed to grow in TAP medium at pH 7.3 (data not shown), implying that specific nutrients present in Allen medium are essential for its growth. These findings highlight the KMJ strain's high degree of acid adaptability

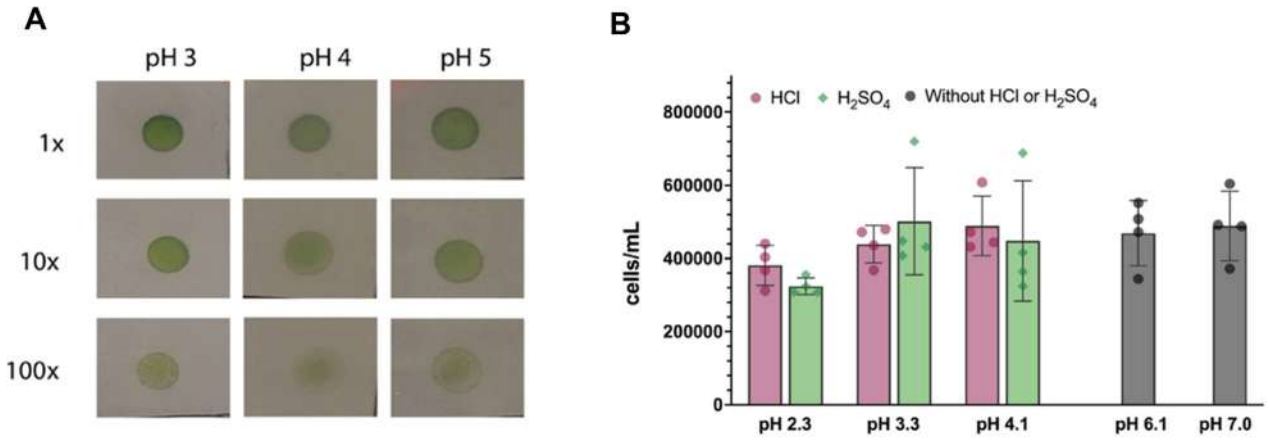

Figure 5. pH tolerance and acid source adaptability of *P. acidicola* strain KMJ. Growth of *P. acidicola* strain KMJ in 1× Allen medium on agar (A) and in liquid medium (B). The pH was adjusted to various levels (2.3–7.0) using HCl (pink) or H_2SO_4 (green) or without acid addition (gray). Cultures were incubated for 9 days, and final cell densities were measured. No significant differences were observed across pH conditions or acid types (two-way ANOVA, $p > 0.05$), indicating broad pH tolerance and anion adaptability. Bars represent mean ± SD from technical replicates (n = 4).

Rates of O_2 evolution (μmol mg chl^{-1} h^{-1})

	10 μM C_i	50 μM C_i	100 μM C_i	4000 μM C_i (V_{max})
C. reinhardtii	43.04 ± 1.17	59.88 ± 0.79	60.5 ± 2.46	69.01 ± 5.94
P. acidicola KMJ	52.45 ± 0.61	72.81 ± 1.93	77.51 ± 4.58	81.20 ± 5.77

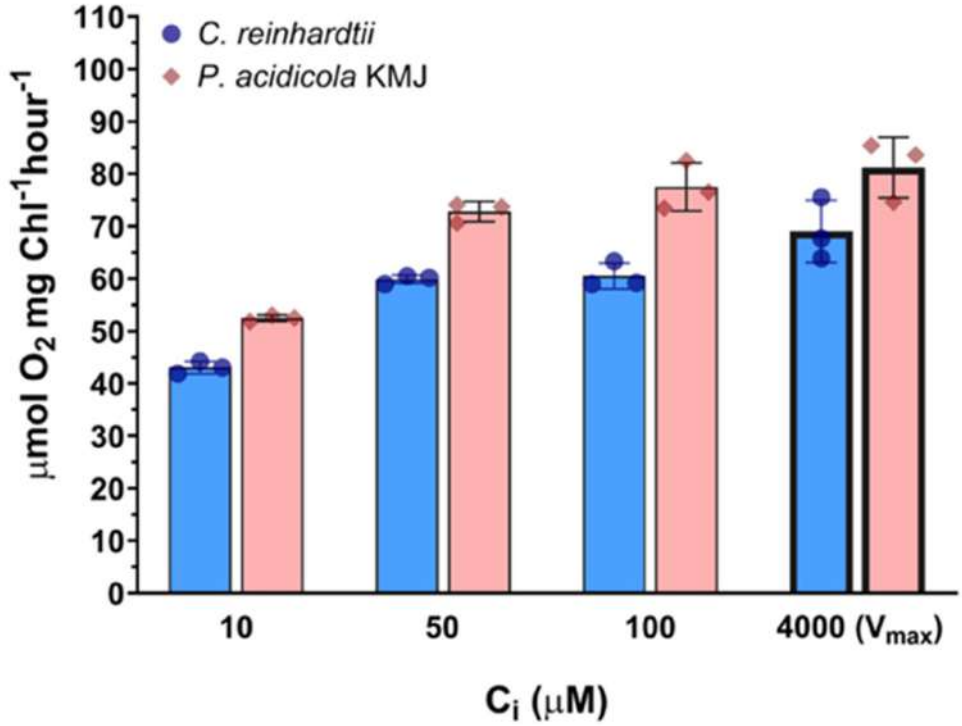

Figure 6. Photosynthetic performance comparison under varying inorganic carbon concentrations. C_i-dependent photosynthetic O_2 evolution rates of *P. acidicola* KMJ (blue) and *C. reinhardtii* (salmon) measured at pH 6 under continuous illumination. Rates were determined at increasing concentrations of inorganic carbon (C_i: 10, 50, 100, and Vmax measured at 4000 μM of C_i). KMJ consistently exhibited higher O_2 evolution rates than *C. reinhardtii* across all conditions. Bars represent mean ± SD from technical replicates (n = 3).

and suggest the presence of metabolic mechanisms that confer resistance to both acidic pH and anion stress, potentially involving sulfur assimilation or detoxification pathways.

Photosynthetic capacity

Given its ability to thrive under extreme pH conditions, we next assessed the photosynthetic performance of *P. acidicola* KMJ to evaluate its light-dependent carbon fixation capacity. The rates of O_2 evolution were measured at pH 6—where CO_2 is the dominant inorganic carbon (C_i: CO_2, HCO_3^-, CO_3^{2-}) species—using varying C_i concentrations (10, 50, 100, and 4000 µM). For comparison, *C. reinhardtii* with an activated CO_2-concentrating mechanism (CCM) was included.

As illustrated in **Figure 6**, *P. acidicola* KMJ exhibited consistently higher O_2 evolution rates than *C. reinhardtii* across all tested concentrations of C_i at pH 6. Under low C_i availability (10–100 µM), *P. acidicola* KMJ maintained notably elevated photosynthetic rates, indicating efficient CO_2 utilization. At 10 µM C_i, KMJ reached 52.45 ± 0.61 µmol O_2 mg^{-1} Chl h^{-1}, compared to 43.04 ± 1.17 µmol O_2 mg^{-1} Chl h^{-1} in *C. reinhardtii*. This advantage persisted at 50 and 100 µM C_i, with *P. acidicola* KMJ achieving 72.81 ± 1.93 and 77.51 ± 4.58 µmol O_2 mg^{-1} Chl h^{-1}, respectively, while *C. reinhardtii* recorded lower rates of 59.88 ± 0.79 and 60.50 ± 2.46 µmol O_2 mg^{-1} Chl h^{-1}. At saturating C_i (4000 µM), the V_max of KMJ (81.20 ± 5.77 µmol O_2 mg^{-1} Chl h^{-1}) remained higher than that of *C. reinhardtii* (69.01 ± 5.94 µmol O_2 mg^{-1} Chl h^{-1}). These results suggest that *P. acidicola* KMJ possesses enhanced capacity for light-driven CO_2 fixation in acidic pH where CO_2 is the dominant C_i species, underscoring its potential for use in low-pH, CO_2-capture applications.

Discussion

The successful isolation of *P. acidicola* KMJ from both the sediment and supernatant fractions of geothermal mud collected at Kamojang underscores the ecological dominance and environmental persistence of this acidophilic microalga within its native habitat. This finding aligns with the known preferences of previously reported *A. protothecoides* var. *acidicola*—recently reclassified as *P. acidicola*—which thrives in extremely low-pH geothermal environments [25, 27]. The 100% sequence identity between isolates from both sediment and supernatant fractions underscores the robustness of the isolation protocol and suggests ecological uniformity of *P. acidicola* within this acidic niche. Although no morphological or physiological differences were observed between fractions, microhabitat heterogeneity was not formally characterized and may still influence population structure. Nonetheless, phylogenetic analysis further supports this interpretation, with KMJ clustering distinctly within the *P. acidicola* lineage and clearly separating from canonical *A. protothecoides*, reinforcing its varietal classification.

We acknowledge that the partial 18S rRNA gene (~500 bp) used in this study provides limited resolution for distinguishing closely related chlorophyte taxa. Notably, the taxonomic reclassification of SAG1951 to *Pumiliosphaera acidicola* was based on ITS-2 sequences [25], which were not included in our current analysis. However, we are currently preparing for whole-genome sequencing (WGS) of strain KMJ. This will allow for robust phylogenomic classification and identification of marker genes involved in acid tolerance and carbon assimilation.

To date, only five 18S rRNA gene sequences of *P. acidicola* are available in GenBank, and no whole-genome sequence has been reported. Moreover, published studies on this taxon remain scarce. These gaps underscore the significance of the current study and highlight the importance of whole-genome sequencing and functional characterization of *P. acidicola* KMJ to better understand its acidophilic adaptations and biotechnological potential.

In parallel with these genomic gaps, physiological evidence also points to the unique acidophilic adaptations of KMJ. The acid tolerance of KMJ is evident in its robust growth on both solid and liquid

media at pH values as low as 2.3—conditions that inhibit the growth of most neutrophilic microalgae, including *Chlorella vulgaris* and *C. reinhardtii* [21, 22]. Although KMJ can grow in Allen medium at neutral pH, it fails to grow in TAP medium under identical conditions. Since TAP is commonly used to culture green algae such as *C. reinhardtii* and *Chlorella* sp., this differential growth likely reflects KMJ's specific dependence on the ionic balance, buffering capacity, or micronutrient composition unique to Allen medium. This observation suggests the presence of auxotrophic traits or specialized nutrient acquisition mechanisms adapted to its native acidic environment.

The comparable growth of KMJ in media acidified with either HCl or H_2SO_4 indicates that its acid tolerance is not limited to a specific acid type. This implies the presence of broad-spectrum acid resistance mechanisms, potentially involving chloride and sulfate ion homeostasis, sulfur metabolism, or enhanced oxidative stress responses. Although acid-tolerant microalgae have been documented in previous studies—such as *Stichococcus bacillaris*, *Chlamydomonas acidophila*, and *G. sulphuraria*, which maintained growth at pH values below 3.0—these investigations typically used sulfuric acid alone and did not explore adaptability across multiple acid sources [28]. Similarly, *Pseudochlorella* sp. YKT1, isolated from sulfuric acid mine drainage, demonstrated optimal growth between pH 3.0 and 5.0 but was also tested only with sulfuric acid [11]. In contrast, KMJ's resilience under both sulfate- and chloride-based acidification distinguishes it from previously reported strains and highlights its ecological versatility.

Such adaptability is advantageous for industrial-scale cultivation in low-pH environments, where contamination risks are inherently reduced. Moreover, KMJ's tolerance—and potential utilization—of sulfate ions may further enhance its applicability in CO_2 capture systems utilizing sulfur-rich flue gases. Although no data on intracellular pH or ion homeostasis were collected in this study, future work will explore these physiological mechanisms to better understand KMJ's acid tolerance. Together, these features position *P. acidicola* KMJ as a robust model for exploring acidophilic adaptation and as a promising chassis for CO_2 capture in challenging environmental conditions.

Beyond its acid tolerance and potential for industrial application, KMJ also demonstrates robust photosynthetic performance under low inorganic carbon availability. Photosynthetic performance in *P. acidicola* KMJ, assessed via O_2 evolution across a gradient of C_i concentrations, exceeded that of *C. reinhardtii* under all tested conditions. At sub-saturating C_i levels (10–100 μM), KMJ exhibited 22–28% higher O_2 evolution rates, suggesting a greater affinity for CO_2 and potentially more efficient CO_2 assimilation. KMJ's O_2 evolution rates approached near-maximum values by 100 μM C_i, with only a modest increase (~5%) up to 4000 μM, indicating efficient CO_2 utilization under low-C_i conditions. Although Km was not explicitly determined, this pattern may reflect a high affinity for CO_2 or a constitutively active uptake system. Alternatively, photosynthetic saturation at low C_i could also indicate downstream metabolic limitations in the Calvin cycle or electron transport chain, which warrant further investigation. In contrast, *C. reinhardtii* showed a more pronounced increase (~14%) over the same range, consistent with its reliance on inducible CO_2-concentrating mechanisms (CCMs). These findings suggest that KMJ may operate a passive or constitutive CO_2 uptake strategy effective under acidic, CO_2-limited environments—possibly involving acid-stable RubisCO isoforms or highly active carbonic anhydrases, though these mechanisms remain to be experimentally verified. To our knowledge, this is the first study to directly quantify C_i-dependent O_2 evolution in an acidophilic chlorophyte, providing new insight into CO_2 assimilation under extreme environmental conditions.

Published studies on other acidophilic photoautotrophs offer context for interpreting these traits. In the red alga *G. sulphuraria*, Oesterhelt et al. [29] reported photosynthetic O_2 evolution at pH 2 with peak rates of ~330 μmol O_2 mg^{-1} Chl h^{-1} under autotrophic conditions. However,

they also observed a shift toward heterotrophy in the presence of glucose, accompanied by PSII inactivation and RubisCO repression. Although our study did not examine the effects of organic substrates, KMJ maintained stable O_2 evolution across a wide Ci range under fully autotrophic conditions. Whether its CO_2 assimilation machinery operates without pre-activation remains unclear and merits further investigation.

Other acid-tolerant microalgae, such as *S. bacillaris*, *C. acidophila*, and *G. sulphuraria*, have been shown to grow below pH 3 [28]. However, photosynthetic rates or C_i-dependent CO_2 fixation were not evaluated. Similarly, *Cyanidioschyzon merolae* has been shown to prefer CO_2 over bicarbonate under acidic conditions, supporting a pH-gradient-based CCM, yet without accompanying data on O_2 evolution or photosynthetic saturation behavior [30].

Taken together, these findings underscore the unique trait combination observed in KMJ: robust growth at low pH (2.3–7.0), efficient photosynthesis across a wide C_i range, and signs of CO_2 fixation saturation at relatively low external CO_2 availability. While the regulatory and energetic mechanisms remain to be resolved, KMJ represents a promising platform for biotechnological CO_2 capture and a valuable model for exploring acidophilic CO_2 assimilation in green algae.

Conclusion

The isolation and characterization of *P. acidicola* KMJ from an Indonesian geothermal spring highlight its exceptional acid tolerance, broad pH adaptability, and efficient photosynthetic performance under variable C_i conditions. KMJ thrives in both chloride- and sulfate-acidified media across a pH range of 2.3–7.0 and maintains high oxygen evolution rates even under low C_i concentrations, outperforming *C. reinhardtii*. These traits, along with its compact cell morphology and ecological robustness, position KMJ as a strong candidate for CO_2 capture technologies in low-pH or sulfur-rich environments. Notably, this study is the first to directly quantify C_i-dependent O_2 evolution in an acidophilic chlorophyte, filling a key gap in the physiological understanding of CO_2 assimilation in acid-tolerant green algae. Beyond its applied potential, KMJ offers a tractable model for exploring the molecular mechanisms of acidophilic photosynthesis and carbon uptake.

Acknowledgment

None.

Funding

This research was supported in part by the Research and Community Service Grant, Pioneer Program, Faculty of Mathematics and Natural Sciences, Institut Teknologi Bandung, 2024 (Grant Number: FMIPA.PPMI-FK-PN-02-2024), and by the Center of Excellence in New and Renewable Energy (PPEBT), Institut Teknologi Bandung, through the Inter-University Center for Excellence (PUAPT) Program funded by the Ministry of Education, Culture, Research, and Technology (Kemdikbudristek), Republic of Indonesia.

Declaration of interest

The authors declare that none of them has any conflict of interest with any private, public or academic party related to the information contained in this manuscript.

Author contributions

AK: Project conception, supervision, O_2 evolution assay, data analysis, visualization, manuscript writing. BGNP: Microalgal isolation, strain confirmation, acid adaptability experiments, data analysis. BAF: Washing and spotting protocol development. AR: Mud sample preparation. RMP, YR: Data analysis. ZN: Project co-conception, supervision, data analysis, field sampling. All authors contributed to manuscript review and approved the final version.

Received: June 1, 2025
Revised: June 10, 2025
Accepted: June 11, 2025
Published: June 23, 2025

References

1. Trends in Atmospheric Carbon Dioxide [Internet]. US Department of Commerce, National Oceanic and Atmospheric Administration. 2025 [cited May 18, 2025]. Available from: https://gml.noaa.gov/ccgg/trends/global.html.
2. Woolway RI, Sharma S, Smol JP. Lakes in Hot Water: The Impacts of a Changing Climate on Aquatic Ecosystems. Bioscience. 2022;72(11):1050-61. https://doi.org/10.1093/biosci/biac052.
3. Wrona FJ, Prowse TD, Reist JD, Hobbie JE, Lévesque LMJ, Vincent WF. Climate Change Effects on Aquatic Biota, Ecosystem Structure and Function. AMBIO: A Journal of the Human Environment. 2006;35(7):359-69, 11. doi: https://doi.org/10.1579/0044-7447(2006)35[359:CCEOAB]2.0.CO;2.
4. Field CB, Behrenfeld MJ, Randerson JT, Falkowski P. Primary Production of the Biosphere: Integrating Terrestrial and Oceanic Components. Science. 1998;281(5374):237-40. https://doi.org/doi:10.1126/science.281.5374.237.
5. Sayre R. Microalgae: The Potential for Carbon Capture. BioScience. 2010;60(9):722-7. https://doi.org/10.1525/bio.2010.60.9.9.
6. Zeng X, Danquah MK, Chen XD, Lu Y. Microalgae bioengineering: From CO_2 fixation to biofuel production. Renewable and Sustainable Energy Reviews. 2011;15(6):3252-60. https://doi.org/10.1016/j.rser.2011.04.014.
7. de Morais MG, Costa JAV. Carbon dioxide fixation by Chlorella kessleri, C. vulgaris, Scenedesmus obliquus and Spirulina sp. cultivated in flasks and vertical tubular photobioreactors. Biotechnology Letters. 2007;29(9):1349-52. https://doi.org/10.1007/s10529-007-9394-6.
8. Qiu R, Gao S, Lopez PA, Ogden KL. Effects of pH on cell growth, lipid production and CO_2 addition of microalgae Chlorella sorokiniana. Algal Research. 2017;28:192-9. https://doi.org/10.1016/j.algal.2017.11.004.
9. Zeebe RE, Wolf-Gladrow D. CO_2 in Seawater: Equilibrium, Kinetics, Isotopes, Chapter 1 Equilibrium. In: Zeebe RE, Wolf-Gladrow D, editors. Elsevier Oceanography Series. 65: Elsevier; 2001. p. 1-84.
10. Trias R, Ménez B, le Campion P, Zivanovic Y, Lecourt L, Lecoeuvre A, et al. High reactivity of deep biota under anthropogenic CO_2 injection into basalt. Nature Communications. 2017;8(1):1063. https://doi.org/10.1038/s41467-017-01288-8.
11. Hirooka S, Higuchi S, Uzuka A, Nozaki H, Miyagishima S-y. Acidophilic Green Alga Pseudochlorella sp. YKT1 Accumulates High Amount of Lipid Droplets under a Nitrogen-Depleted Condition at a Low-pH. PLOS ONE. 2014;9(9):e107702. https://doi.org/10.1371/journal.pone.0107702.
12. Dean AP, Hartley A, McIntosh OA, Smith A, Feord HK, Holmberg NH, et al. Metabolic adaptation of a Chlamydomonas acidophila strain isolated from acid mine drainage ponds with low eukaryotic diversity. Science of The Total Environment. 2019;647:75-87. https://doi.org/10.1016/j.scitotenv.2018.07.445.
13. Delmelle P, Bernard A. Geochemistry, mineralogy, and chemical modeling of the acid crater lake of Kawah Ijen Volcano, Indonesia. Geochimica et Cosmochimica Acta. 1994;58(11):2445-60. https://doi.org/10.1016/0016-7037(94)90023-X.
14. Aditiawati P, Yohandini H, Madayanti F, Akhmaloka. Microbial Diversity of Acidic Hot Spring (Kawah Hujan B) in Geothermal Field of Kamojang Area, West Java-Indonesia. The Open Microbiology Journal. 2009;3:121–8. https://doi.org/10.2174/1874285800903010058.
15. Allen MB. Studies with Cyanidium caldarium, an anomalously pigmented chlorophyte. Arch Mikrobiol. 1959;32(3):270-7. https://doi.org/10.1007/bf00409348.
16. Gross W, Schnarrenberger C. Heterotrophic Growth of Two Strains of the Acido-Thermophilic Red Alga Galdieria sulphuraria. Plant and Cell Physiology. 1995;36(4):633-8. https://doi.org/10.1093/oxfordjournals.pcp.a078803.
17. Chen CC, Bates R, Carlson J. Effect of environmental and cultural conditions on medium pH and explant growth performance of Douglas-fir (Pseudotsuga menziesii) shoot cultures. F1000Res. 2014;3:298. https://doi.org/10.12688/f1000research.5919.2.
18. Kono A, Spalding MH. LCI1, a Chlamydomonas reinhardtii plasma membrane protein, functions in active CO_2 uptake under low CO_2. The Plant Journal. 2020;102(6):1127-41. doi: https://doi.org/10.1111/tpj.14761.
19. Cao M, Fu Y, Guo Y, Pan J. Chlamydomonas (Chlorophyceae) colony PCR. Protoplasma. 2009;235(1-4):107-10. https://doi.org/10.1007/s00709-009-0036-9.
20. Madeira F, Madhusoodanan N, Lee J, Eusebi A, Niewielska A, Tivey ARN, et al. The EMBL-EBI Job Dispatcher sequence analysis tools framework in 2024. Nucleic Acids Res. 2024;52(W1):W521-W5. https://doi.org/10.1093/nar/gkae241
21. Ronquist F, Teslenko M, van der Mark P, Ayres DL, Darling A, Höhna S, et al. MrBayes 3.2: Efficient Bayesian Phylogenetic Inference and Model Choice Across a Large Model Space. Systematic Biology. 2012;61(3):539-42. https://doi.org/10.1093/sysbio/sys029.
22. Rambaut A. FigTree v1.4.4. Institute of Evolutionary Biology, University of Edinburgh; 2009.
23. Gorman DS, Levine RP. Cytochrome f and plastocyanin: their sequence in the photosynthetic electron transport chain of Chlamydomonas reinhardi. Proc Natl Acad Sci U S A. 1965;54(6):1665-9. https://doi.org/10.1073/pnas.54.6.1665
24. Wintermans JFGM, De Mots A. Spectrophotometric characteristics of chlorophylls a and b and their phenophytins in ethanol. Biochimica et Biophysica Acta (BBA) - Biophysics including Photosynthesis. 1965;109(2):448-53. https://doi.org/10.1016/0926-6585(65)90170-6.

25. Darienko T, Pröschold T. Genetic variability and taxonomic revision of the genus Auxenochlorella (Shihira et Krauss) Kalina et Puncocharova (Trebouxiophyceae, Chlorophyta). Journal of Phycology. 2015;51(2):394-400. https://doi.org/10.1111/jpy.12279.

26. Li X, Hou Z, Xu C, Shi X, Yang L, Lewis LA, et al. Large Phylogenomic Data sets Reveal Deep Relationships and Trait Evolution in Chlorophyte Green Algae. Genome Biology and Evolution. 2021;13(7). https://doi.org/10.1093/gbe/evab101.

27. Johnson DB. Acidophilic algae isolated from mine-impacted environments and their roles in sustaining heterotrophic acidophiles. Frontiers in Microbiology. 2012;Volume 3 - 2012. https://doi.org/10.3389/fmicb.2012.00325.

28. Abiusi F, Trompetter E, Pollio A, Wijffels RH, Janssen M. Acid Tolerant and Acidophilic Microalgae: An Underexplored World of Biotechnological Opportunities. Frontiers in Microbiology. 2022;Volume 13 - 2022. https://doi.org/10.3389/fmicb.2022.820907.

29. Oesterhelt C, Schmälzlin E, Schmitt JM, Lokstein H. Regulation of photosynthesis in the unicellular acidophilic red alga Galdieria sulphuraria†. The Plant Journal. 2007;51(3):500-11. https://doi.org/10.1111/j.1365-313X.2007.03159.x.

30. Steensma AK, Shachar-Hill Y, Walker BJ. The carbon-concentrating mechanism of the extremophilic red microalga Cyanidioschyzon merolae. Photosynthesis Research. 2023;156(2):247-64. https://doi.org/10.1007/s11120-023-01000-6.